Ion-Beam Induced Surface Roughening of Poly-(methyl methacrylate) (PMMA) Tuned by a Mixture of Ar and O_2 Ions

Wei Dai, Tae-Jun Ko, Kyu Hwan Oh, Kwang-Ryeol Lee, Myoung-Woon Moon*

The evolution of ion-beam induced surface roughening of PMMA was investigated using an anode-layer ion beam source with O_2, Ar, and their mixture. Use of the O_2 ion beam created rough granular patterns on the surface of PMMA because O_2 ions could break the C–C backbone and subsequently combine with the broken C bonds, resulting in local cross-linking and aggregation. However, the Ar ion beam tended to reduce the surface roughness due to the decomposition of the oxygen-containing ester groups (O–CH_3 and O–C=O) and the increase of an overall cross-linking of the amorphous carbon layer, which played a role in etch resistance and suppression of polymer mobility as well as aggregation on the modified PMMA surface. By varying the ratio of Ar over O_2, the surface morphology of PMMA was modified to exhibit features ranging from granular roughness to crater-like features.

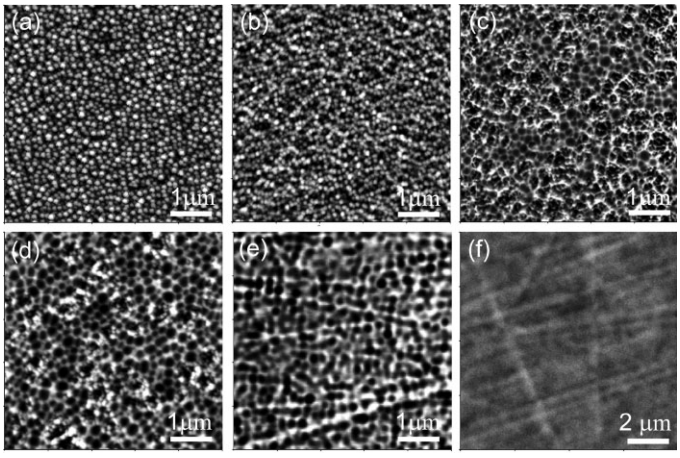

1. Introduction

With its outstanding optical transparency, attractive electrical and mechanical properties, and good compatibility with human tissue, poly-(methyl methacrylate) (PMMA), a transparent thermoplastic, has been investigated for use in various applications, such as optical windows and lenses, medical technologies and implants, and microfluidics and biochips.[1–4] To extend the applications of PMMA, surface modification, such as plasma and/or ion-beam treatments, has been studied to alter the chemical, mechanical, and optical properties by tuning the chemical functionality or physical morphology of the surface. For example, Schulz et al.[5,6] reported that antireflective structures generated on PMMA by plasma treatment exhibited reduced surface reflection. In addition, Tsougeni et al.[7] reported the nanotexturing of PMMA using oxygen plasma treatment for protein microarray applications and found that the nanotextured PMMA, which has a high surface area, significantly increased protein adsorption compared to an untreated PMMA surface. Thus, surface roughening controlled by either plasma or ion-beam treatments can be used to improve the

W. Dai, T.-J. Ko, K.-R. Lee, M.-W. Moon
Future Convergence Technology Research Division, Korea Institute of Science and Technology, Seoul 130-650, Republic of Korea
E-mail: mwmoon@kist.re.kr
T.-J. Ko, K. H. Oh
Department of Materials Science and Engineering, Seoul National University, Seoul 151-742, Republic of Korea

DOI: 10.1002/ppap.201200037

functionality of PMMA substrates without affecting the bulk properties.

Both plasma and ion-beam treatments of polymeric materials have been demonstrated as methods for altering the surface chemistry and for physical roughening of the surface by producing patterns of various shapes, such as a ripple, dot, hole, pillar, and hair, which depend on the nature of the polymer.[8–11] During plasma or ion-beam exposures, energetic ion bombardment can break the polymer backbone and cause the scission and depolymerization of the side chains, thereby altering the collective (or selective) etching behavior of the irradiated material.[12,13] Furthermore, chain cross-linking and recombination and polymer aggregation are expected to occur, which affect the surface roughening and texturing of the polymer.[14,15] The process conditions, including the species and the energies of the bombarding ions, have a dramatic influence on the chain cross-linking and scission. Reactive-gas ions, such as, O_2 ions, were found to enhance local cross-linking and aggregation at polymer surfaces due to the formation of polar functional groups, such as carbonyl and carbonate groups, while an inert Ar ion beam or plasma was reported to decompose the ester group of PMMA, leading to enhanced surface smoothness.[16–18] Accordingly, controlling the surface features of PMMA was achievable by the counter influences of local aggregation due to reactive-gas ions (like O_2 ion) treatment and flattening due to inert Ar ion treatment.

In this paper, we used O_2, Ar, and O_2/Ar mixtures ion beams to modify the PMMA surface to tune surface features by introducing the relevant gas (O_2, Ar, or a mixture of the two) into a linear ion source, which can be scaled to any desired length up to the meter scale and has already been widely used to treat large-area substrate surfaces in industrial applications.[19] The evolution of the PMMA surface topography and chemistry induced by ion-beam treatment was carefully investigated as a function of treatment duration and substrate bias voltage, as well as the gas flow ratios of oxygen and argon in the gas mixtures. The relationship between processing, surface chemistry and surface topography in ion beam-treated PMMA was studied systematically. The overall objective is to develop a better understanding of the ion-beam induced surface roughening of PMMA and subsequently to control the surface features.

2. Experimental Section

The surface-roughening process was performed in an anode-layer linear ion beam source. The flat coupons of PMMA (LG Chem.,

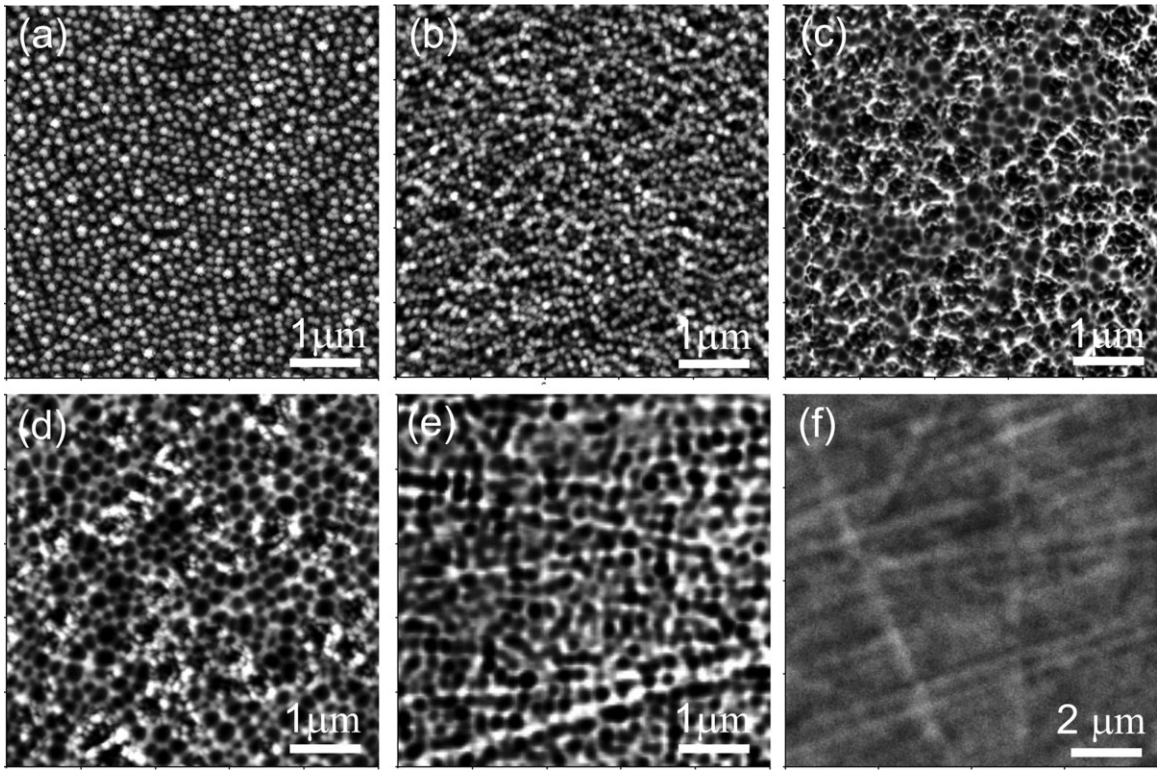

Figure 1. AFM images of the surface topography of PMMA treated by ion beams for 30 min at a bias voltage of −200 V and with different flow rate ratios: (a) 15 sccm O_2, (b) O_2/Ar = 2.0 (10 sccm/5 sccm), (c) O_2/Ar = 1.0 (7.5/7.5), d) O_2/Ar = 0.5 (5/10), e) O_2/Ar = 0.25 (3/12), and d) 15 sccm Ar. Note that the black spots shown in (c), (d), and (e) indicate a hole- or crater-like feature.

DOI: 10.1002/ppap.201200037

Rep. of Korea) with sizes of $30 \times 30 \times 4\,mm^3$ were placed into a vacuum chamber, which was evacuated to a base pressure of approximately 2×10^{-5} Torr. The distance between the ion source and the substrate holder is approximately 150 mm. The single gases (O_2 or Ar) and the gas mixtures of O_2 and Ar with ratios of 2.0 (10 sccm/5 sccm), 1.0 (7.5/7.5), 0.5 (5/10), and 0.25 (3/12), were introduced into the anode of the ion source to produce the Ar and O_2 ions. The total gas flow rate was maintained at 15 sccm. During the process, the deposition temperature was lower than 60 °C, and the work pressure was maintained at approximately 5×10^{-5} Torr. The discharge voltage was maintained at a constant value of 1.4 kV with a discharge current of 0.2 A. A radio frequency (r.f.) bias voltage, which was applied to the substrate holder, was varied from −200 to −800 V in order to vary the ion beam energy.[20,21] The process duration was varied from 1 to 30 min.

The surface morphology of the treated PMMA was measured using an atomic force microscope (AFM, XE-70, Park systems) in non-contact mode at a scan rate of 0.5 Hz. The root-mean-square (RMS) roughness R_q of the film surfaces was calculated from $1\,024 \times 1\,024$ surface height data points obtained from $10\,\mu m \times 10\,\mu m$ scan areas.[22] The bond details of the treated PMMA were characterized using Raman spectroscopy with incident light from a Xe^+ laser at a wavelength of 532 nm. The Raman scattering range was from 400 to $4\,000\,cm^{-1}$. Compositional analysis was performed using XPS to investigate the chemical change of the PMMA surface by ion beam treatment. An Al K_α (1 486.6 eV) X-ray source was used as the excitation source for XPS, and the X-ray source anode was maintained at 250 W, 10 kV, and 27 mA with a beam spot size of $400\,\mu m \times 400\,\mu m$. The XPS peak position was calibrated using the C1s peak at 284.6 eV.

3. Results and Discussion

Figure 1 shows the topographical evolution of the ion beam-treated PMMA as a function of the ratio of O_2 and Ar with the sample at a bias voltage of −200 V. The surface of the PMMA treated by a pure O_2 ion beam typically exhibited granular roughness features with a lateral size of approximately 100 nm, as shown in Figure 1a. The granular structure features became small and difficult to distinguish as Ar gas was added to produce the mixture gas of O_2/Ar = 10/5 or 2.0, as shown in Figure 1b. As the flow rate ratio of O_2 and Ar decreased to 7.5/7.5 or 1.0, crater-like features began to appear on the surface of the treated PMMA, as shown in Figure 1c, and the surface became increasingly smooth as the flow rate ratio was reduced to 5/10 or 0.5. However, when the ratio decreased even further (O_2/Ar = 3/12 or 0.25), the craters started to disappear. For the pure Ar ion beam treatment, the treated PMMA exhibited a smooth surface that did not have any characteristic features. These observations indicate that the morphological features on the PMMA surface can be tuned by varying the Ar and O_2 ratio in the precursor gas mixtures for the ion beam source.

Figure 2 presents the typical topographies of the PMMA etched by ion beams with various ratios of the O_2 and Ar gas mixtures as a function of the treatment duration, which

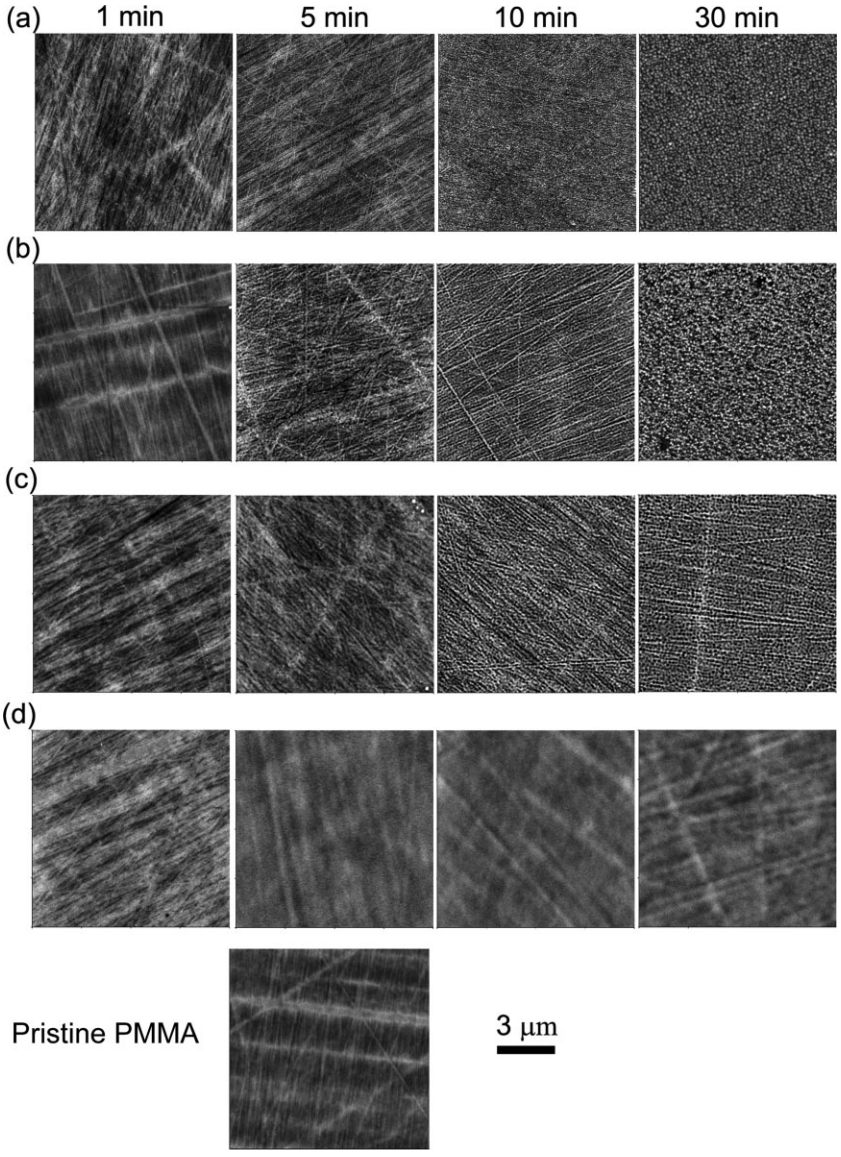

Figure 2. Typical AFM images of the surface topography of PMMA treated by exposure to ion beams with various O_2/Ar flow rate ratios and treatment durations at a bias voltage of −200 V: (a) 15 sccm O_2, (b) O_2/Ar = 2, (c) O_2/Ar = 0.5, and (d) 15 sccm Ar.

varied from 1 to 30 min, at the bias voltage of −200 V. The surface of the PMMA treated by the O_2 ion beam became increasingly rough, with a higher number of granular features appearing with an increase of the treatment duration, as shown in Figure 2a. Apparently, the roughening process can be divided into two stages. For the initial stage (treatment duration ≤5 min), cone-shaped features increased gradually in number on the surface. However, because the cone-shaped features are very small, the treated PMMA maintained a smooth surface, with a low RMS roughness of approximately 1 nm, which is similar to the value for the pristine PMMA surface (see Figure 3). When the treatment time was further increased (>5 min), aggregated hillocks began to form on the surface, with the lateral size and amplitude of the patterns increasing with the treatment duration, reaching values of about 100 and 200 nm, respectively, at 30 min of exposure. Simultaneously, the formation of the granular features corresponded to the increase of the RMS roughness up to 64 nm. The surface evolution of the PMMA treated by mixtures of O_2 and Ar ion beams exhibited similar behavior to that of the PMMA treated by an O_2 ion beam, as shown in Figure 2b and c. However, it should be noted that the surface of the treated PMMA became increasingly smooth with increasing Ar fraction in the gas mixture (see Figure 2d). The surface roughness of the PMMA samples treated by the ion beam source with various ratios of the Ar and O_2 mixture are shown in Figure 3. Note that the overall shape of the roughness-to-treatment-duration curves is similar for all flow rate ratios of the Ar and O_2 gases for the ion beam source. During the initial stage, all of the treated PMMA exhibited a smooth surface with low RMS roughness. However, when the treatment duration increased further (>5 min), although the roughness also increased with the treatment duration, the growth rate of the roughness dramatically decreased with increasing the Ar fraction in the gas mixture for the same treatment duration. Note that the RMS roughness of the PMMA treated using only the Ar ion beam exhibited an opposite change to that treated with the Ar and O_2 mixture and showed a small decrease from ≈1 to 0.5 nm with the treatment duration, as shown in an inset of Figure 3. It is clear that the polymer aggregation plays a significantly role in the roughness formation. During the O_2 or O_2/Ar mixtures ion beam treatments, the surface of PMMA tends to aggregate and resulting in an increase of the roughness. However, it seemed that a smooth modified-layer was formed on the PMMA by Ar ion beam treatment, which caused the decrease in the surface roughness.

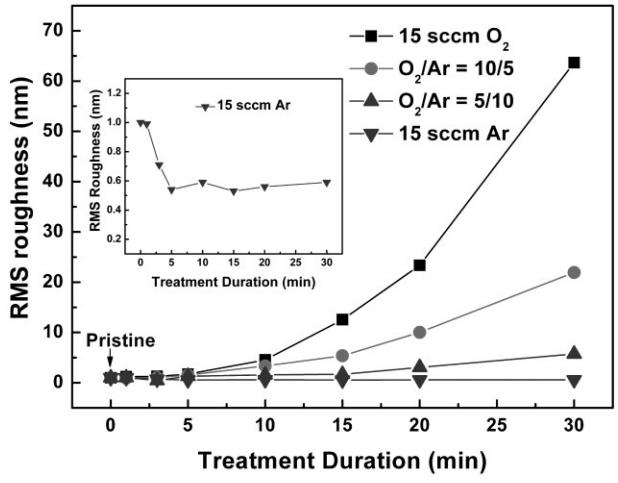

Figure 3. RMS surface roughness of the PMMA treated by ion beam exposure with various O_2/Ar flow rate ratios as a function of the treatment duration at a bias voltage of −200 V.

XPS analysis, which is a semi-quantitative spectroscopic technique that simultaneously has high surface-sensitivity, was used to characterize the change in the surface chemistry of the ion beam-treated PMMA compared with the pristine PMMA. Figure 4a and b show the C 1s spectra of the PMMA treated by an O_2 ion beam and an Ar ion beam, respectively. Generally, the C 1s spectra of the pristine PMMA (as shown in Figure 4a) can be deconvoluted into three components with binding energies of 284.5, 286.1, and 288.5 eV, corresponding to C−C−H bonds, methoxy group (O−CH_3) of the ester chemical function, and carboxylic group (O−C=O), respectively, in the PMMA monomer.[23] When the surface of the PMMA samples were treated by ion beams, the structures of the C 1s spectra were greatly affected. For the O_2 ion beam treated PMMA, it is characteristic to note that the intensity of the C 1s spectra around 287.2 eV show a distinctive increase compared with that of the pristine PMMA. Indeed, the decomposition of the C 1s peak reveals a new peak at binding energy of about 287.1 eV, which could be attributed to the new functional group, C−OH bond. The formation of the C−OH new group can be also illustrated in O 1s spectra as shown in Figure 5. The O 1s spectrum of the pristine PMMA can be deconvoluted in two typical peaks around 531.7 and 533.2 eV, which correspond to C−O and C−O−C bonds in ester group of PMMA, respectively. However, besides the two peaks above, the O 1s spectra of the PMMA treated O_2 ion beam reveals the presence of one new component around 532.4 eV, which can be assigned to the C−OH group.[24,25] On the other hand, for the Ar ion beam treated PMMA, the high binding energy side (around 288.5 eV) of the C 1s spectra shows losses of intensity, implying the reduction of oxygen-containing groups (O−CH_3 and O−C−O). The C−OH group was also observed in the decomposition of the C 1s peaks. It was reported that −OH group could be also generated during Ar plasma treatments.[25]

The relative peak areas of the fitted peaks of Figure 4a and b are presented in Figure 4c and d, respectively. As shown in

DOI: 10.1002/ppap.201200037

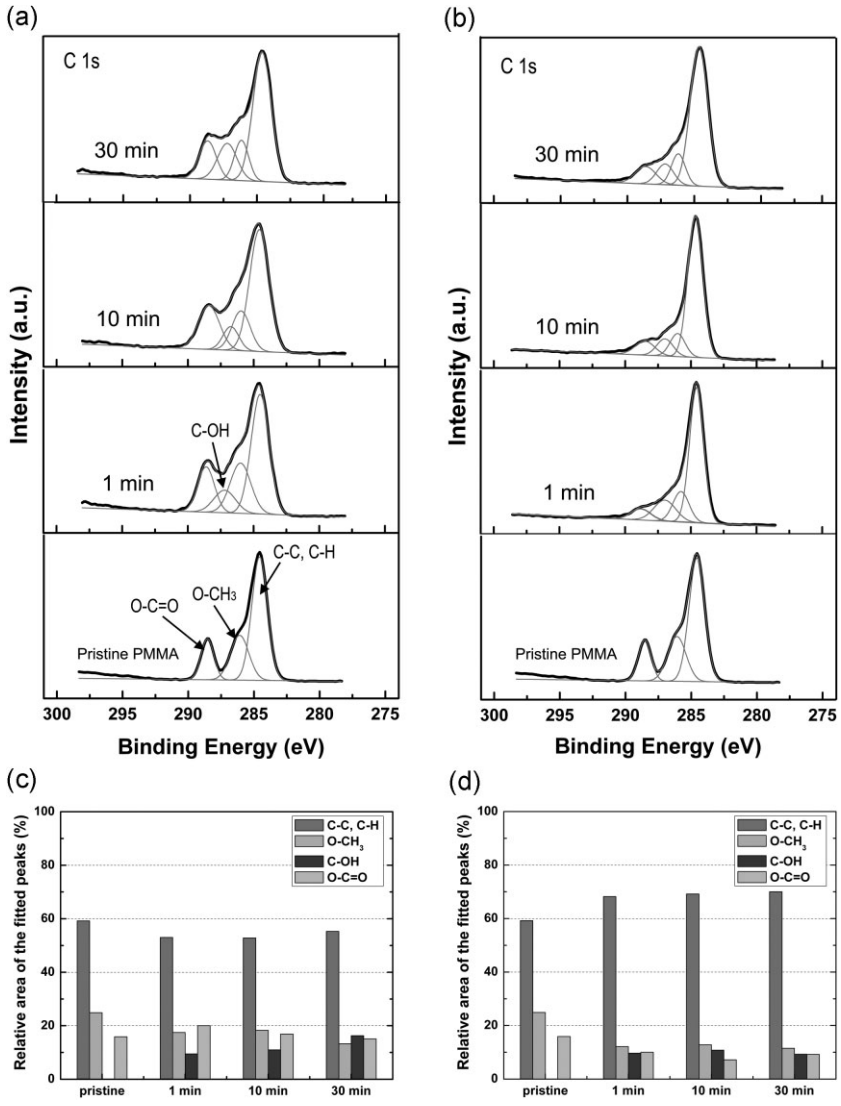

Figure 4. Typical XPS C 1s peaks of the PMMA treated by (a) O_2 ions and (b) Ar ions; (c) and (d) are the relative peak areas of the fitted peaks in a) and b), respectively.

Figure 4c, the peak proportion of the C–C (and CH) and O–CH_3 functionalities of the PMMA treated by an O_2 ion beam exhibited a decrease compared with that of the pristine PMMA. Simultaneously, a certain amount of C–OH functionalities were formed with the O_2 ion beam treatment. This observation can be explained by the breaking of the backbone C–C chain and of O–CH_3 groups by O_2 ions, which result in the formation of dangling bonds susceptible to react with O_2 ions; this, in turn, increases the number of C–OH bonds. For the Ar ion beam treated PMMA, the peak proportion of the C–C (and C–H) bonds exhibited an increase compared with that of the pristine PMMA, while the peak contributions of the O–CH_3 and O–C–O groups decreased. This reduction of the peak contributions can be attributed to the Ar ion bombardment, which is expected to cause degradation of the polymer surface with preferential elimination of the oxygen-containing group as volatile carbon monoxide or dioxide followed by the formation of C–C bonds.[26]

Raman spectroscopy is a reliable tool for the characterization of carbon materials, and thus, it has also been used to characterize the details of the bond structural changes of the treated PMMA.[27] Figure 6 presents the Raman shift of the PMMA by O_2 and Ar ion beams as a function of the treatment duration. The Raman spectrum of the PMMA treated by O_2 ion beam exposure for 1 min becomes broader and shows a new peak in the 1 000–1 700 cm^{-1} region compared to that of pristine PMMA (see Figure 6a). Generally, amorphous carbon materials, such as a-C:H, exhibit a Raman scattering band with a broad asymmetry in the range from 1 000 to 1 700 cm^{-1}, which originates from the composition of two sp^2 carbon bands: the G-band (G-peak) at 1 580 cm^{-1} corresponding to C–C stretching vibrations and the D-band (D-peak) at 1 360 cm^{-1} corresponding to the symmetric breathing vibration of the aromatic carbon rings.[27,28] The presence of the broad peak in the range from 1 000 to 1 700 cm^{-1} indicates the formation of an amorphous carbon modified layer on PMMA by the ion beam treatment. However, as the O_2 ion beam treatment duration increased further, the new broad peak disappeared. This disappearance may be attributed to oxidation of the amorphous carbon by the O_2 ions, which easily remove the carbon modified layer by reacting with the carbon to produce volatile species. In contrast, for Ar ion beam treatment (shown in Figure 6b), the broad peak between 1 000 and 1 700 cm^{-1} became wider and stronger as the treatment duration was increased, which implies that the fraction of the carbon phase induced by the Ar ion beam increased with increasing the treatment duration. This result is similar to the XPS analysis that demonstrated that a large number of C–C and C–H bonds were formed by the Ar ion beam treatment, and that those bonds are likely due to the amorphous carbon-modified layer, as amorphous hydrocarbon materials also have a characteristic C 1s XPS spectrum at the binding energy of approximately 284.5 eV.[27,29] Figure 6c shows the Raman

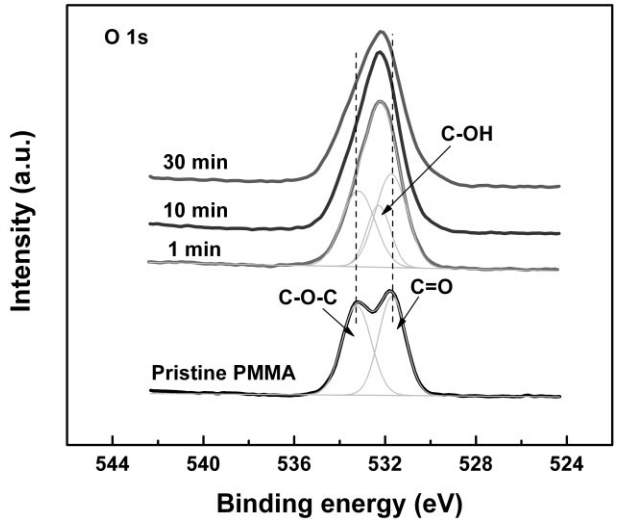

Figure 5. Typical XPS O 1s peaks of the PMMA treated by O_2 ion beam.

spectra of the PMMA treated with various gas mixtures of O_2 and Ar for 30 min. It can be seen that the broad peak in the region of 1 000–1 700 cm^{-1} grows larger and increases gradually as the Ar fraction in the gas mixture increases, indicating that more amorphous carbon was formed on the PMMA surface due to the Ar ion addition in the ion beam treatment.

Both the XPS and Raman analyses suggest that the O_2 ion beam tends to break the C—C backbone, creating radicals which subsequently react with other C- or O-radicals, resulting in local cross-linking and polymer aggregation. Consequently, the granular roughness features are formed, as shown in Figure 1a. Unlike the O_2 ion beam treatment, the Ar ion beam treatment seems to favor the decomposition of the oxygen-containing ester group and subsequently formation of C—C and C—H bonds, thus giving rise to overall cross-linking of the amorphous carbon modified layer, which exhibits similarities due to the ion beam-induced layers on polymers.[9,29–32] The overall cross-linked modified layer is expected to suppress polymer mobility and aggregation, thereby decreasing the surface roughness.[14,33] Accordingly, the PMMA treated by the Ar ion beam exhibited a very low roughness of approximately 0.5 nm, as shown in Figure 1f, while the PMMA treated by the O_2 ion beam exhibited a high roughness of approximately 64 nm, as shown in Figure 1. Furthermore, by tuning the counter-influences of local aggregation due to O_2 ion beam treatment and the flattening or smoothening due to Ar ion beam treatment, the PMMA surface can be modified to exhibit characteristic features, ranging from granular to crater-like features, by tuning the flow rate ratio.

The etch rate of the PMMA after ion beam treatment is also consistent with the formation of the overall cross-linked amorphous carbon modified layer that provides etch

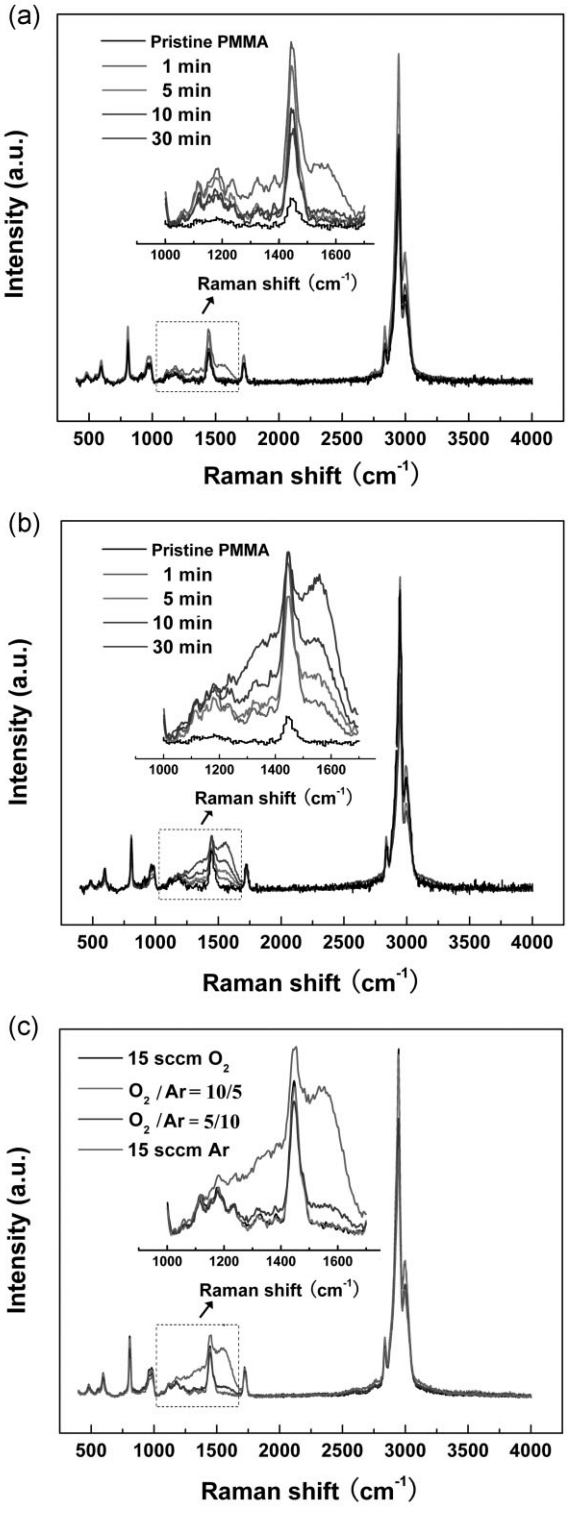

Figure 6. Raman spectra of PMMA: (a) treated by an O_2 ion beam at different treatment durations, (b) treated by an Ar ion beam at different treatment durations, and (c) treated by ion beams with various O_2/Ar flow rate ratios for 30 min.

DOI: 10.1002/ppap.201200037

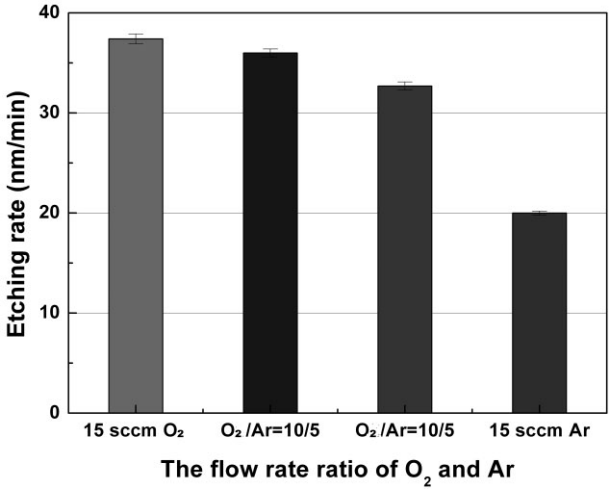

Figure 7. Etch rates of PMMA treated by ion beam exposure with various O_2/Ar flow rate ratios.

resistance.[14,30,34] Figure 7 shows the etch rates of the PMMA treated by various gas mixtures feeding the ion beam source. The etch rate of the PMMA treated by an Ar ion beam was measured to be a relatively low value of $\approx 20\ nm \cdot min^{-1}$ due to the protection by the amorphous carbon modified layer. However, when an O_2 ion beam was used, the C–C bonds are broken in the carbon modified layer, which enhances the depolymerization of the C–C backbone chains. As a result, the PMMA etch rate increases as the ratio of O_2/Ar increases, and it reaches $37\ nm \cdot min^{-1}$ for PMMA treated with a pure O_2 ion beam.

In addition to the influence of the flow rate ratios of the ion beam, the influence of the substrate bias voltage on the roughening of the PMMA surface was also studied. Figure 8 shows the AFM topographies of the PMMA samples treated by Ar and O_2 ion beams for 10 min at various bias voltages, which were quantified with an RMS roughness value, as shown in Figure 9. For the PMMA treated by an O_2 ion beam, although the network structures were observed at high voltage, the structure definition began to disappear as the bias voltage increased from −200 to −800 V, and the roughness of the PMMA treated by O_2 ion beam was reduced sharply from ≈4.5 to 1.8 nm. For the samples treated by an Ar ion beam, however, as the bias voltage increased, the surface roughness exhibited a small increase from ≈0.5 to 1 nm.

The Raman spectra of ion beam-treated PMMA samples under different bias voltages are shown in Figure 10. For the PMMA treated by O_2 ion beam exposure, the G-peak centered at approximately $1\,580\ cm^{-1}$ increased slightly with an increase of the bias voltage (see Figure 10a), which indicates that some amorphous carbon was formed on the PMMA surface. The previously described results at an applied bias of −200 V indicate that oxidization inhibits the formation of an amorphous carbon modified layer on the PMMA surface by O_2 ion beam treatment. Thus, the appearance of the amorphous carbon detected on the PMMA surface at high bias voltage may be due to the high energy ion bombardment, which would enhance the overall cross-linking, and thus result in the formation of an amorphous carbon modified layer and therefore cause the

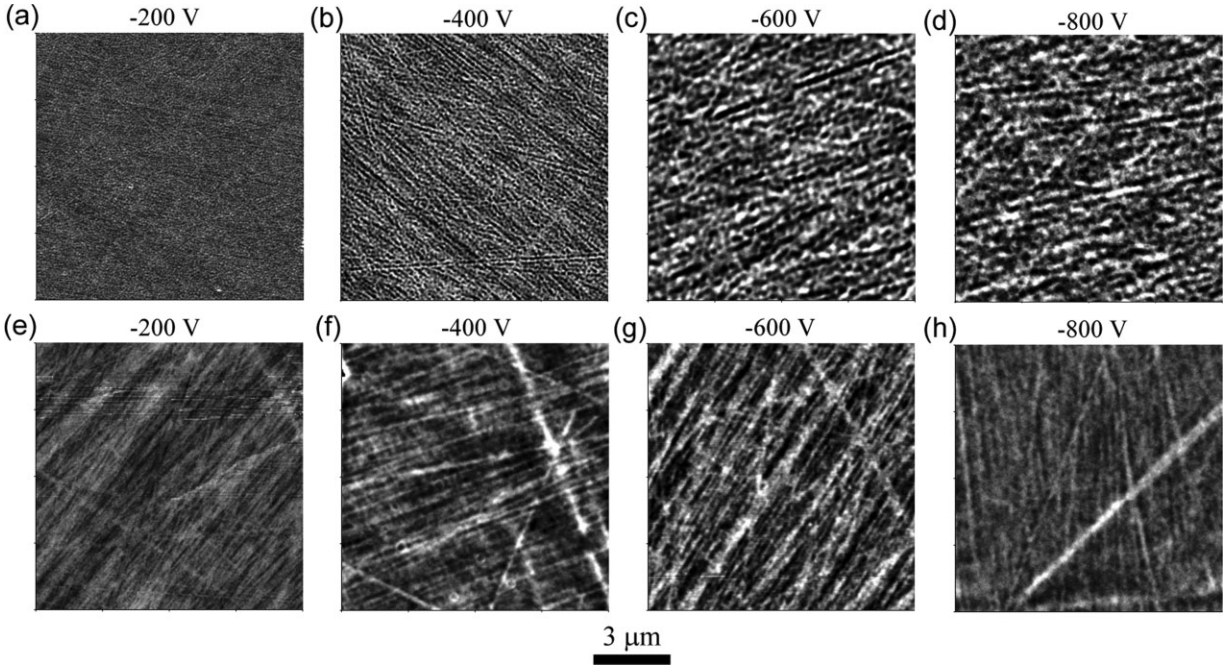

Figure 8. Surface topography of PMMA treated by ion beams exposure for 10 min at different bias voltages: (a–d) O_2 ion beam and (e–h) Ar ion beam.

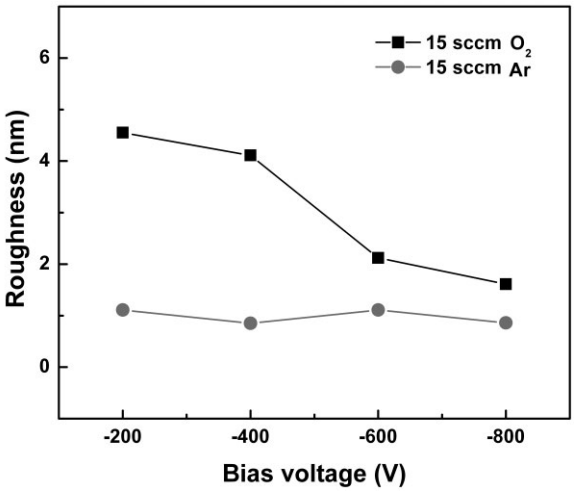

Figure 9. Surface roughness of the PMMA treated by ion beams for 10 min as a function of bias voltage.

observed reduction of the surface roughness.[33] In contrast, the opposite trend of the G-peak intensity was observed for PMMA treated by an Ar ion beam. As shown in Figure 10b, the G-peak decreased as the bias voltage increased, i.e., the fraction of the amorphous carbon decreased with increasing bias voltage.[20] Therefore, Ar ion irradiation, while it induces chain decomposition and results in the carbonization of the surface and the formation of the amorphous carbon modified layer, sputters the newly formed amorphous carbon away as the Ar ions bombard the PMMA surface,[30,34] i.e., there is a balance between carbonization and sputtering during etching. With a high bias voltage, the sputtering effect is enhanced, resulting in a decrease in the fraction of the amorphous carbon due to sputtering of the surface layer. However, some amorphous carbon remains on the PMMA surface, so PMMA treated by an Ar ion beam also exhibited a smooth surface and insignificant roughness at high bias voltage. Compared with the effect of the flow rate ratio, the bias voltage had a smaller effect on the roughening of the PMMA surface.

4. Conclusion

PMMA was treated by ions from an anode-layer ion-beam source with various O_2/Ar source gas flow rate ratios as a function of the treatment duration. Based on XPS and Raman spectroscopy results, the O_2 ion beam is found to break the C—C backbone, and the oxygen ions are found to react with C radicals to form a new C—OH groups. Consequently, local cross-linking and aggregation occurs, resulting in granular features on the PMMA surface that exhibit high roughness. However, use of the Ar ion beams favor the decomposition of the oxygen-containing ester group (O—CH_3 and O—C—O) and an overall cross-linking to form an amorphous carbon modified-layer, which suppresses polymer aggregation and thus decreases the surface roughness. The gas mixture of inert Ar and reactive O_2 ions could cause the counter influences of local aggregation and smoothness on the PMMA surface, respectively, to form tunable features evolving from granular to crater-like configurations. Thus, the surface topography of the PMMA can be controlled by varying the Ar and O_2 ratio in the gas mixture supplying the ion source. In addition, the increase of the bias voltage enhances the overall cross-linking and reduces the surface roughness, but it exhibited a smaller

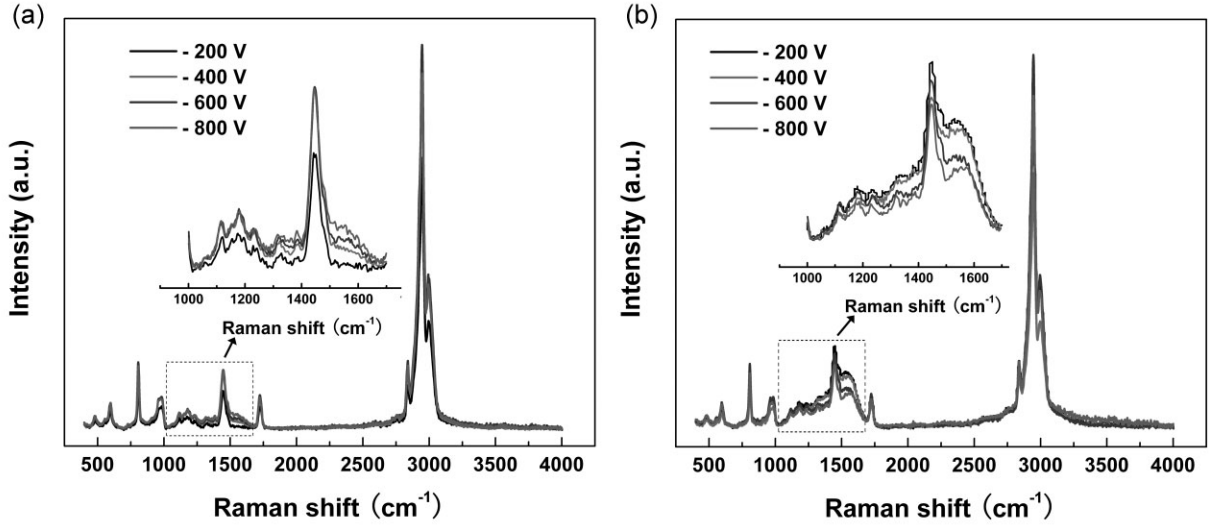

Figure 10. Raman spectra of the PMMA treated by ion beam exposure for 10 min at different bias voltages: a) O_2 ion beam and b) Ar ion beam.

DOI: 10.1002/ppap.201200037

effect on the roughening of PMMA compared with the effect of varying the mixture of the gas species of Ar and O_2.

Acknowledgements: This work was financially supported in part by TES Co. Ltd. under the "Advanced Manufacturing Technology Research Center" Program of the MKE of Korea (KRL) and in part by the MKE of Korea through the Fundamental R&D Program for Core Technology of Materials (MWM) and a KIST internal project.

Received: March 14, 2012; Revised: May 15, 2012; Accepted: May 27, 2012; DOI: 10.1002/ppap.201200037

Keywords: amorphous carbon; nanopatterns; PMMA; polymer treatments; surface roughness

[1] C. Ozcan, N. Hasirci, *J. Biomater. Sci., Polym. Ed.* **2007**, *18*, 759.
[2] J. B. Lhoest, J. L. Dewez, P. Bertrand, *Nucl. Instrum. Methods Phys. Res., Sect. B* **1995**, *105*, 322.
[3] U. Schulz, P. Munzert, N. J. Kaiser, *Surf. Coat. Technol.* **2001**, *142/144*, 507.
[4] M. Yoshinari, T. Kato, K. Matsuzaka, T. Hayakawa, T. Inoue, Y. Oda, M. Shimono, *J. Biomed. Mater. Res., B Appl. Biomater.* **2006**, *77*, 47.
[5] U. Schulz, P. Munzert, N. Kaiser, *J. Adhes. Sci. Technol.* **2010**, *24*, 1283.
[6] A. Kaless, U. Schulz, P. Munzert, N. Kaiser, *Surf. Coat. Technol.* **2005**, *200*, 58.
[7] K. Tsougeni, A. Tserepi, V. Constantoudis, E. Gogolides, *Langmuir* **2010**, *26*, 13883.
[8] M. W. Moon, S. H. Lee, J. Y. Sun, K. H. Oh, A. Vaziri, J. W. Hutchinson, *Proc. Natl. Acad. Sci. USA* **2007**, *104*, 1130.
[9] E. K. Her, H. S. Chung, M. W. Moon, K. H. Oh, *Nanotechnology* **2009**, *20*, 285301.
[10] S. F. Ahmed, K. R. Lee, J. Yoon, M. W. Moon, *Appl. Surf. Sci.* **2012**, *258*, 3841.
[11] B. Shin, K. R. Lee, M. W. Moon, H. Y. Kim, *Soft Matter* **2012**, *8*, 1817.
[12] T. Y. Chung, D. Nest, D. B. Graves, F. Weilnboeck, R. L. Bruce, G. S. Oehrlein, D. Wang, M. Li, E. A. Hudson, *J. Phys. D: Appl. Phys.* **2010**, *43*, 272001.
[13] M. C. Coen, R. Lehmann, P. Groening, L. Schlapbach, *Appl. Surf. Sci.* **2003**, *207*, 276.
[14] Y. Ting, C. Liu, S. Park, H. Jiang, P. F. Nealey, A. E. Wendt, *Polymer* **2010**, *2*, 649.
[15] T. Yoshimura, H. Shiraishi, J. Yamamoto, T. Terasawa, *Appl. Phys. Lett.* **1996**, *68*, 1799.
[16] J. Chai, F. Lu, B. Li, D. Kwok, *Langmuir* **2004**, *20*, 10919.
[17] P. Gröning, O. M. Küttel, M. Collaud-Coen, G. Dietler, L. Schlapbach, *Appl. Surf. Sci.* **1995**, *89*, 83.
[18] P. Gröning, M. Collaud, G. Dietler, L. Schlapbach, *J. Appl. Phys.* **1994**, *76*, 887.
[19] A. Anders, *Surf. Coat. Technol.* **2005**, *200*, 1893.
[20] R. K. Roy, S. K. F. Ahmed, J. W. Yi, M. W. Moon, K. R. Lee, Y. Jun, *Vacuum* **2009**, *83*, 1179.
[21] S. F. Ahmed, J. W. Yi, M. W. Moon, Y. J. Jang, B. H. Park, S. H. Lee, K. R. Lee, *Plasma Process. Polym.* **2009**, *6*, 860.
[22] H.-S. Zhang, J. L. Endrino, A. Anders, *Appl. Surf. Sci.* **2008**, *255*, 2551.
[23] S. W. Rosencrance, W. K. Way, N. Winograd, D. A. Shirley, *Surf. Sci. Spectra* **1993**, *2*, 71.
[24] S. Massey, D. Roy, A. Adnot, *Nucl. Instrum. Methods Phys. Res., Sect. B* **2003**, *208*, 236.
[25] S. Ben Amor, G. Baud, M. Jacquet, G. Nansé, P. Fioux, M. Nardin, *Appl. Surf. Sci.* **2000**, *153*, 172.
[26] R. Nathawat, A. Kumar, N. K. Acharya, Y. K. Vijay, *Surf. Coat. Technol.* **2009**, *203*, 2600.
[27] J. Robertson, *Mater. Sci. Eng., R* **2002**, *37*, 129.
[28] C. Casiraghi, A. C. Ferrari, J. Robertson, *Phys. Rev. B* **2005**, *72*, 085401.
[29] W. Dai, G. Wu, A. Wang, *Diamond Relat. Mater.* **2010**, *19*, 1307.
[30] J. J. Végh, D. Nest, D. B. Graves, R. Bruce, S. Engelmann, T. Kwon, R. J. Phaneuf, G. S. Oehrlein, B. K. Long, C. G. Willson, *J. Appl. Phys.* **2008**, *104*, 034308.
[31] B. K. Gan, M. M. M. Bilek, A. Kondyurin, K. Mizuno, D. R. McKenzie, *Nucl. Instrum. Methods Phys. Res., Sect. B* **2006**, *247*, 254.
[32] E. Pargon, K. Menguelti, M. Martin, A. Bazin, O. Chaix-Pluchery, C. Sourd, S. Derrough, T. Lill, O. Joubert, *J. Appl. Phys.* **2009**, *105*, 094902.
[33] S. F. Tead, W. E. Vanderlinde, G. Marra, A. L. Ruoff, E. J. Kramer, F. D. Egitto, *J. Appl. Phys.* **1990**, *68*, 2972.
[34] A. Kondyurin, M. Bilek, *Nucl. Instrum. Methods Phys. Res., Sect. B* **2011**, *269*, 1361.